Constraining warm dark matter candidates including sterile neutrinos and light gravitinos with WMAP and the Lyman-α forest

Matteo Viel,[1] Julien Lesgourgues,[2,3] Martin G. Haehnelt,[1] Sabino Matarrese,[4,3] and Antonio Riotto[3]

[1]*Institute of Astronomy, Madingley Road, Cambridge CB3 0HA, United Kingdom*
[2]*Laboratoire de Physique Théorique LAPTH, F-74941 Annecy-le-Vieux Cedex, France*
[3]*INFN, Sezione di Padova, Via Marzolo 8, I-35131 Padova, Italy*
[4]*Dipartimento di Fisica "G. Galilei," Università di Padova, Via Marzolo 8, I-35131 Padova, Italy*

(Received 28 January 2005; published 31 March 2005)

The matter power spectrum at comoving scales of $(1-40)h^{-1}$ Mpc is very sensitive to the presence of Warm Dark Matter (WDM) particles with large free-streaming lengths. We present constraints on the mass of WDM particles from a combined analysis of the matter power spectrum inferred from the large samples of high-resolution high signal-to-noise Lyman-α forest data of Kim *et al.* (2004) and Croft *et al.* (2002) and the cosmic microwave background data of WMAP. We obtain a lower limit of $m_{\rm WDM} \gtrsim 550$ eV (2σ) for early decoupled thermal relics and $m_{\rm WDM} \gtrsim 2.0$ keV (2σ) for sterile neutrinos. We also investigate the case where in addition to cold dark matter a light thermal gravitino with fixed effective temperature contributes significantly to the matter density. In that case the gravitino density is proportional to its mass, and we find an upper limit $m_{3/2} \lesssim 16$ eV (2σ). This translates into a bound on the scale of supersymmetry breaking, $\Lambda_{\rm susy} \lesssim 260$ TeV, for models of supersymmetric gauge mediation in which the gravitino is the lightest supersymmetric particle.

DOI: 10.1103/PhysRevD.71.063534 PACS numbers: 98.80.Cq

I. INTRODUCTION

It is now observationally well established that the Universe is close to flat and that matter accounts for about (25–30) percent of the total energy density most of which must be in the form of dark matter (DM) particles. Candidates of dark matter particles are generally classified according to their velocity dispersion which defines a free-streaming length. On scales smaller than the free-streaming length, fluctuations in the dark matter density are erased and gravitational clustering is suppressed. The velocity dispersion of Cold Dark Matter (CDM) particles is by definition so small that the corresponding free-streaming length is irrelevant for cosmological structure formation. That of Hot Dark Matter (HDM), e.g. light neutrinos, is only 1 or 2 orders of magnitude smaller than the speed of light, and smooths out fluctuations in the total matter density even on galaxy cluster scales, which leads to strong bounds on their mass and density [1–3]. Between these two limits, there exists an intermediate range of dark matter candidates generically called Warm Dark Matter (WDM). If such particles are initially in thermal equilibrium, they decouple well before ordinary neutrinos. As a result their temperature is smaller and their free-streaming length shorter than that of ordinary neutrinos. For instance, thermal relics with a mass of order 1 keV and a density $\Omega_x \sim 0.25$ would have a free-streaming length comparable to galaxy scales ($\lambda_{\rm FS} \sim 0.3$ Mpc).

There exist many WDM candidates whose origin is firmly rooted in particle physics. A prominent example is the gravitino, the supersymmetric partner of the graviton. The gravitino mass $m_{3/2}$ is generically of the order of $\Lambda_{\rm susy}/M_p$, where $\Lambda_{\rm susy}$ is the scale of supersymmetry breaking and M_p is the Planckian scale. If $\Lambda_{\rm susy}$ is large the Lightest Supersymmetric Particle (LSP), which is then not the gravitino, decouples in the nonrelativistic regime and provides a viable CDM candidate. If, however, $\Lambda_{\rm susy} \lesssim 10^6$ GeV, as predicted by theories where supersymmetry breaking is mediated by gauge interactions, the gravitino is likely to be the LSP. Such a light gravitino has a wide range of possible masses (from 10^{-6} eV up to the keV region). The gravitino—or better to say its helicity 1/2 component—decouples when it is still relativistic. At this time the number of degrees of freedom in the Universe is typically of order 100, much larger than at neutrino decoupling. The effective gravitino temperature is therefore always smaller than the neutrino temperature, and such light gravitinos can play the role of WDM [4]. Their velocity dispersion is non-negligible during the time of structure formation, but smaller than the velocity dispersion of active neutrinos with the same mass.

Other particles may decouple even earlier from thermal equilibrium while still relativistic and may act as warm dark matter. The same is true for right-handed or sterile neutrinos added to the standard electroweak theory. Since their only direct coupling is to left-handed or active neutrinos, the most efficient production mechanism is via neutrino oscillations. If the production rate is always less than the expansion rate, then these neutrinos will never be in thermal equilibrium. However, enough of them may be produced to account for the observed matter density. Right-handed (sterile) neutrinos with a mass of order keV are therefore natural WDM candidates [5,6].

The suppression of structures on scales of a Mpc and smaller, in WDM models with a particle mass of ~1 keV,

has been invoked as a possible solution to two major apparent conflicts between CDM models and observations in the local Universe (see [7–10] and references therein). The first problem concerns the inner mass density profiles of simulated dark matter halos that are generally more cuspy than inferred from the rotation curves of many dwarfs and low surface brightness galaxies. Secondly, N-body simulations of CDM models predict large numbers of low mass halos greatly in excess of the observed number of satellite galaxies in the Local Group. It appears, however, difficult to find WDM parameters which solve all apparent CDM problems simultaneously and it is also not clear whether the tension between theory and observations is due to an inappropriate comparison of numerical simulations and observational data. The main difficulty is that the modeling of the inner density profile of galaxies and the abundance of satellite galaxies requires simulations on scales where the matter density field is highly nonlinear at low redshift. Furthermore, many of the relevant baryonic processes are poorly understood.

At $z \sim (2-3)$ the gravitational clustering of the matter distribution spectrum at scales larger than the free-streaming length of a thermal 1 keV WDM particle is still in the mildly nonlinear regime. At these redshift high-resolution Lyman-α forest data offer an excellent probe of the matter power spectrum at these scales. Narayanan *et al.* [10] compared the flux power spectrum and flux probability distribution of a small sample of high-resolution quasar (QSO) absorption spectra to that obtained from numerical dark matter simulations. In this way they were able to constrain the mass of a thermal WDM particle (assumed to account for all the dark matter in the Universe) to be $m_{\rm WDM} \gtrsim 750$ eV.

We will use here the linear DM power spectrum inferred from two large samples of QSO absorption spectra [11,12] using state-of-the-art hydrodynamical simulations [13] combined with cosmic microwave background data from WMAP in order to obtain new constraints on the mass of possible thermally distributed WDM particles. We thereby assume that WDM particles account for all the DM in our Universe and we do not put any priors on their temperature. We will also further investigate constraints on the mass of light gravitinos with realistic effective temperature.

The paper is organized as follows. In Section II we will describe the effect of WDM on the power spectrum of the matter distribution. In Section III we will summarize the method used in inferring the linear matter power spectrum from Lyman-α forest observations and discuss the systematic errors involved. In Section IV A we will derive a lower limit for the mass of the dark matter particle in a pure ΛWDM model. In Section IV B, we will obtain an upper limit for the mass of light gravitinos in a mixed ΛCWDM universe. Section V contains our conclusions and some comments on the implications of our results for particle physics.

II. WDM SIGNATURES ON THE MATTER POWER SPECTRUM

Standard neutrinos are believed to decouple from the plasma when they are still relativistic, slightly before electron-positron annihilation. They will keep the equilibrium distribution of a massless fermion with temperature $T_\nu \simeq (4/11)^{1/3} T_\gamma$. Their total mass summed over all neutrino species and their density are related through the well-known relation $\Omega_\nu h^2 \simeq (m_\nu/94\ \text{eV})$ in the instantaneous decoupling limit. This result does, however, not apply to WDM for which: (i) either decoupling takes place earlier, or (ii) the particles were never in thermal equilibrium.

If decoupling takes place at temperature T_D while there are $g_*(T_D)$ degrees of freedom the particles do not share the entropy release from the successive annihilations and their temperature is suppressed today by a factor

$$\frac{T_x}{T_\nu} = \left(\frac{10.75}{g_*(T_D)}\right)^{1/3} < 1, \tag{1}$$

as is the case e.g. for gravitinos. If the particles have never been in thermal equilibrium, there is a wide range of possible models. We will restrict our analysis here to the case of sterile neutrinos created from oscillations with active neutrinos, which share the same phase-space distribution but with an overall suppression factor χ. In both cases, the number density of WDM is smaller than that of standard neutrinos, and the same presentday nonrelativistic energy density corresponds to a larger particle mass,

$$\omega_x = \Omega_x h^2 = \beta\left(\frac{m_x}{94\ \text{eV}}\right), \tag{2}$$

with $\beta = (T_x/T_\nu)^3$ for early decoupled thermal relics and $\beta = \chi$ for sterile neutrinos. Because of their free-streaming velocity, WDM particles slow down the growth of structure and suppress the total matter power spectrum $P(k)$ on scales smaller than their free-streaming scale which is roughly given by

$$k_{\rm FS} = \frac{2\pi}{\lambda_{\rm FS}} \sim 5\ \text{Mpc}^{-1}\left(\frac{m_x}{1\ \text{keV}}\right)\left(\frac{T_\nu}{T_x}\right), \tag{3}$$

see e.g. [14]. Note, however, that there exist different definitions of the free-streaming or damping scale. The effect of the free streaming on the matter distribution can be described by a relative "transfer function,"

$$T(k) = [P(k)_{\Lambda\rm WDM}/P(k)_{\Lambda\rm CDM}]^{1/2} \tag{4}$$

which is simply the square root of the ratio of the matter power spectrum in the presence of WDM to that in the presence of purely cold dark matter, for fixed cosmological parameters.

Since we allowed for an arbitrary normalization factor χ, the three parameters ω_x, m_x, and T_x are independent. Note, however, that the evolution equations for WDM as well as the corresponding terms in the Einstein equations

can be reparametrized entirely in terms of two parameters, for instance ω_x and m_x/T_x (where T_x is expressed in units of the neutrino or photon temperature). There is a simple one-to-one correspondence between the masses of thermal WDM particles and sterile neutrinos for which the effect on the matter distribution and thus the transfer function for both models are identical [6]. Writing Eq. (2) in the two cases and equating ω_x and m_x/T_x, one obtains

$$m_{\text{sterile }\nu} = 4.43 \text{ keV}\left(\frac{m_{\text{thermal}}}{1\text{keV}}\right)^{4/3}\left(\frac{0.25(0.7)^2}{\omega_x}\right)^{1/3}. \quad (5)$$

In the following, we will thus consider only the thermal model and simply translate any mass limit into that for the sterile neutrinos using Eq. (5).

Let us now discuss briefly some simple scenarios.

Pure warm dark matter models—In the case in which the Universe contains only WDM (in addition to the usual baryon, radiation, and cosmological constant components), the transfer function can be approximated by the fitting function [7]

$$T(k) = [1 + (\alpha k)^{2\nu}]^{-5/\nu} \quad (6)$$

where α, the scale of the break, is a function of the WDM parameters, while the index ν is fixed. With a Boltzmann code simulation (using either CMBFAST [15] or CAMB [16]), we find that $\nu = 1.12$ is the best fit for $k < 5h$ Mpc^{-1} and we obtain

$$\alpha = 0.24\left(\frac{m_x/T_x}{1 \text{ keV}/T_\nu}\right)^{-0.83}\left(\frac{\omega_x}{0.25(0.7)^2}\right)^{-0.16}\text{Mpc}$$
$$= 0.049\left(\frac{m_x}{1 \text{ keV}}\right)^{-1.11}\left(\frac{\Omega_x}{0.25}\right)^{0.11}\left(\frac{h}{0.7}\right)^{1.22} h^{-1} \text{ Mpc} \quad (7)$$

where the second line applies only to the case of thermal relics. This expression is close to that of [7] (and exactly identical to the results of [17], except for the front factor which was misprinted in this reference).

In Fig. 1, we plot the results of the numerical simulations and compare them with our analytical fit. The power spectrum of the ΛWDM model differs from that of the corresponding ΛCDM model only at small scales. This is the reason why WDM has been suggested as a solution to the apparent ''crisis'' of CDM models on small scales. The matter density is fixed by the CMB and other data to $\omega_x \sim 0.12$. For pure ΛWDM models for which $m_x \sim 1$ keV this gives $g_*(T_D) \sim 10^3$. The particles therefore decouple extremely early in such a model. Note that the light gravitino suggested by gauge-mediated models of supersymmetry breaking decoupled when g_* was much smaller, of the order of 100.

Mixed models with CDM and gravitinos (or any thermal relics with $g_*(T_D)$ of a hundred)—We will now consider the case of thermal relics which decoupled at a temperature when $g_*(T_D) \sim 100$, as e.g. the light gravitino, which is likely to be the LSP in gauge-mediated theories of supersymmetry breaking. Note that $g_*(T_D) \sim 100$ corresponds to a decoupling temperature between a few GeV and a few TeV (possibly much higher, depending on which theory is assumed beyond the standard model). Note further that the temperature of thermal relics with $g_*(T_D) \sim 100$ is about a factor two smaller than that of ordinary neutrinos. They are thus not equivalent to HDM even in the small mass limit. For fixed g_*, both the density ω_x and the free-streaming wave number are proportional to the mass m_x. Taking $g_* = 100$, one gets

$$\omega_x = 0.117\frac{m_x}{100 \text{ eV}}, \qquad k_{\text{FS}} \sim 1.5h \text{ Mpc}^{-1}\frac{m_x}{100 \text{ eV}}. \quad (8)$$

In the absence of any cold dark matter, the preferred value $\omega_x \sim 0.12$ would lead to a mass of order 100 eV and to a complete smoothing out of fluctuations for $k > 1.5h$ Mpc^{-1}, at odds with the Lyman-α forest data (and with various other constrains related to structure formation [18]). However, in the presence of CDM, small-scale structures are not completely suppressed and the free-

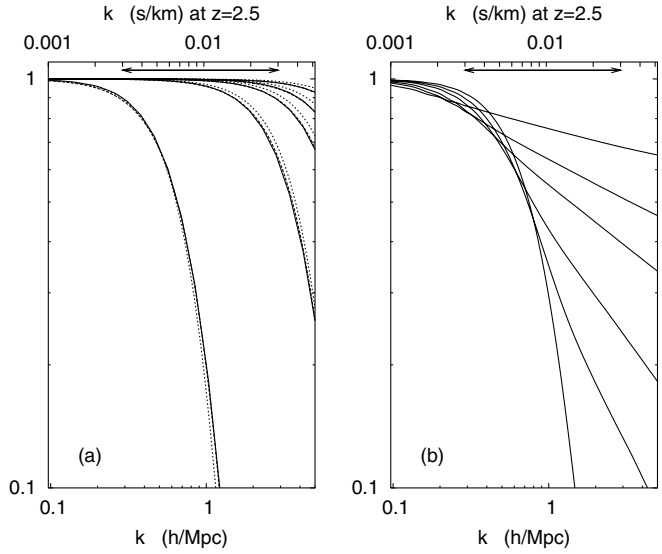

FIG. 1. The WDM transfer function $T(k)$ defined in Eq. (4) for various models (all with the same cosmological parameters $\Omega_B = 0.05$, $\Omega_{DM} = 0.25$, $\Omega_\Lambda = 0.70$). (a) Pure ΛWDM model with, from left to right, $T_x/T_\nu = 0.5$, 0.3, 0.25, 0.226, 0.2, corresponding to $m_x = 92$, 427, 738, 1000, 1441 eV. The solid curves are obtained numerically, the long-dashed curves (essentially indistinguishable from the solid curves) show the analytical fits based on Eq. (7), the short-dashed curves those based on Ref. [7]. (b) Mixed ΛCWDM model for a warm component which decoupled when $g_*(T_D) = 100$, like e.g. a light gravitino (with mass proportional to density and $\Omega_{\text{CDM}} = 0.25 - \Omega_x$). The solid curves show the numerical results for $m_x = 10$, 20, 30, 50, 70, 100 eV, from top right to bottom left. At the top axis we show the wave number scale in s/km (assuming the above cosmological model and $z = 2.5$ intermediate between the two Lyman-α data sets analyzed here). In both panels the double arrow indicates the range of wave numbers used in our analysis.

streaming effect leads to a steplike transfer function (as for massive neutrinos, but with a step at a much smaller scale), while in the small m_x limit standard ΛCDM is recovered. For a light gravitino in the mass range 10 eV $\lesssim m_{3/2} \lesssim$ 100 eV, $g_*(T_D)$ varies between 87 and 101 depending on the details of the supersymmetric model [18]. As we already pointed out a light gravitino with larger mass would result in a matter density which exceeds that observed and as we will show later smaller masses are hard to constrain with current observations. In Fig. 1 we show the transfer function computed numerically for a few values of the mass in the range (10–100) eV, corresponding to $k_{\rm FS}$ in the range (0.15-1.5)h Mpc^{-1}. Since the matter power spectrum measured from galaxy redshift surveys can be compared to linear predictions up to $k \sim 0.15h$ Mpc, it has little sensitivity to this model but as we will show in Section IV the matter power spectrum inferred from Lyman-α data provides a tight upper limit on the gravitino mass.

Mixed models with warmer thermal relics—Finally, the WDM particles could decouple at temperature of order 1 GeV or below (i.e. just before or after the QCD phase transition), when the number of degrees of freedom was in the range $10.75 < g_* < 80$ leading later to a temperature $0.5 < (T_x/T_\nu) < 1$. This case smoothly interpolates between that of ordinary neutrinos (HDM) and that of the previous paragraph. The free-streaming wave number is smaller than for the gravitino and these models have been constrained by the matter power spectrum reconstructed from galaxy redshift surveys [3]. We will not consider this case here.

III. PROBING THE MATTER POWER SPECTRUM WITH THE LYMAN-α FOREST IN QSO ABSORPTION SPECTRA

It is well established by analytical calculation and hydrodynamical simulations that the Lyman-α forest blueward of the Lyman-α emission line in QSO spectra is produced by the inhomogenous distribution of a warm ($\sim 10^4$ K) and photoionized intergalactic medium (IGM) along the line-of-sight. The opacity fluctuations in the spectra arise from fluctuations in the matter density and trace the gravitational clustering of the matter distribution in the quasilinear regime [19]. The Lyman-α forest has thus been used extensively as a probe of the matter power spectrum on comoving scales of $(1-40)h^{-1}$ Mpc [12,13,19,20].

The Lyman-α optical depth in velocity space u (km/s) is related to the neutral hydrogen distribution in real space as (e.g. Ref. [21]):

$$\tau(u) = \frac{\sigma_{0,\alpha} c}{H(z)} \int_{-\infty}^{\infty} dy\, n_{\rm HI}(y) \mathcal{V}[u - y - v_\parallel(y), b(y)] dy, \tag{9}$$

where $\sigma_{0,\alpha} = 4.45 \times 10^{-18}$ cm^2 is the hydrogen Lyα cross section, y is the real-space coordinate (in km s^{-1}), $\mathcal{V}$ is the standard Voigt profile normalized in real space, $b = (2k_B T/mc^2)^{1/2}$ is the velocity dispersion in units of c, $H(z)$ the Hubble parameter, $n_{\rm HI}$ is the local density of neutral hydrogen, and $v_\parallel$ is the peculiar velocity along the line-of-sight. The density of neutral hydrogen can be obtained by solving the photoionization equilibrium equation (e.g. [22]). The neutral hydrogen in the IGM responsible for the Lyman-α forest absorptions is highly ionized due to the metagalactic ultraviolet (UV) background radiation produced by stars and QSOs at high redshift. This optically thin gas in photoionization equilibrium produces a Lyman-α optical depth of order unity.

The balance between the photoionization heating by the UV background and adiabatic cooling by the expansion of the Universe drives most of the gas with $\delta_b < 10$, which dominates the Lyman-α opacity, onto a power-law density relation $T = T_0(1+\delta_b)^{\gamma-1}$, where the parameters T_0 and γ depend on the reionization history and spectral shape of the UV background and δ_b is the local gas overdensity ($1 + \delta_b = \rho_b/\bar{\rho}_b$).

The relevant physical processes can be readily modeled in hydrodynamical simulations. The physics of a photoionized IGM that traces the dark matter distribution is, however, sufficiently simple that considerable insight can be gained from analytical modeling of the IGM opacity based on the so-called Fluctuating Gunn Peterson Approximation neglecting the effect of peculiar velocities and the thermal broadening [23]. The Fluctuating Gunn Peterson Approximation makes use of the power-law temperature-density relation and describes the relation between Lyman-α opacity and gas density (see [12,24]) along a given line-of-sight as follows,

$$\tau(z) \propto (1+\delta_b(z))^2 T^{-0.7}(z) = \mathcal{A}(z)(1+\delta_b(z))^\beta,$$
$$\mathcal{A}(z) = 0.433 \left(\frac{1+z}{3.5}\right)^6 \left(\frac{\Omega_b h^2}{0.02}\right)^2 \left(\frac{T_0}{6000\ \rm K}\right)^{-0.7} \left(\frac{h}{0.65}\right)^{-1} \times \left(\frac{H(z)/H_0}{3.68}\right)^{-1} \left(\frac{\Gamma_{\rm HI}}{1.5\times 10^{-12}{\rm s}^{-1}}\right)^{-1}, \tag{10}$$

where $\beta \equiv 2 - 0.7(\gamma - 1)$ in the range 1.6–1.8, $\Gamma_{\rm HI}$ the HI photoionization rate, $H_0 = h100$ km/s/Mpc the Hubble parameter at redshift zero. For a quantitative analysis, however, full hydrodynamical simulations, which properly simulate the nonlinear evolution of the IGM and its thermal state, are needed.

Eqs. (9) and (10) show how the observed flux $F = \exp(-\tau)$ depends on the underlying local gas density ρ_b, which in turn is simply related to the dark matter density, at least at large scales where the baryonic pressure can be neglected [25]. Statistical properties of the flux distribution, such as the flux power spectrum, are thus closely related to the statistical properties of the underlying matter density field.

A. The data: from the quasar spectra to the flux power spectrum

The power spectrum of the observed flux in high-resolution Lyman-α forest data provides meaningful constraints on the dark matter power spectrum on scales of $0.003\ \mathrm{s/km} < k < 0.03\ \mathrm{s/km}$, roughly corresponding to scales of $(1-40)h^{-1}$ Mpc (somewhat dependent on the cosmological model). At larger scales the errors due to uncertainties in fitting a continuum (i.e. in removing the long wavelength dependence of the spectrum emitted by each QSO) become very large while at smaller scales the contribution of metal absorption systems becomes dominant (see e.g. [11,26]). In this paper, we will use the dark matter power spectrum that Viel, Haehnelt, and Springel [13] (VHS) inferred from the flux power spectra of the Croft *et al.* [12] (C02) sample and the LUQAS sample of high-resolution Lyman-α forest data [27]. The C02 sample consists of 30 Keck high-resolution HIRES spectra and 23 Keck low-resolution LRIS spectra and has a median redshift of $z = 2.72$. The LUQAS sample contains 27 spectra taken with the UVES spectrograph and has a median redshift of $z = 2.125$. The resolution of the spectra is 6 km/s, 8 km/s, and 130 km/s for the UVES, HIRES, and LRIS spectra, respectively. The S/N per resolution element is typically 30–50. Damped and subdamped Lyman-α systems have been removed from the LUQAS sample and their impact on the flux power spectrum has been quantified by [12]. Estimates for the errors introduced by continuum fitting, the presence of metal lines in the forest region, and strong absorptions systems have also been made [11,12,26,28].

We stress that the total sample that went into the estimate of the linear power spectrum used here is about 10 times larger than the one used in the study by [10].

B. From the flux power spectrum to the linear matter power spectrum

VHS have used numerical simulation to calibrate the relation between flux power spectrum and linear dark matter power spectrum with a method proposed by C02 and improved by [29] and VHS. A set of hydrodynamical simulations for a coarse grid of the relevant parameters is used to find a model that provides a reasonable but not exact fit to the observed flux power spectrum. It is then assumed that the differences between the model and the observed linear power spectrum depend linearly on the matter power spectrum.

The hydrodynamical simulations are used to define a bias function between flux and matter power spectrum: $P_F(k) = b^2(k)P(k)$, on the range of scales of interest. In this way the linear matter power spectrum can be recovered with reasonable computational resources. This method has been found to be robust provided the systematic uncertainties are properly taken into account [13,29]. Running hydrodynamical simulations for a fine grid of all the relevant parameters is unfortunately computationally prohibitive.

The use of state-of-the-art hydrodynamical simulations is a significant improvement compared to previous studies which used numerical simulation of dark matter only [10,12]. We use a new version of the parallel TreeSPH code GADGET [30] in its TreePM mode which speeds up the calculation of long-range gravitational forces considerably. The simulations are performed with periodic boundary conditions with an equal number of dark matter and gas particles. Radiative cooling and heating processes are followed using an implementation similar to [22] for a primordial mix of hydrogen and helium. The UV background is given by [31]. In order to maximize the speed of the simulation a simplified criterion of star formation has been applied: all the gas at overdensities larger than 1000 times the mean overdensity is turned into stars [13]. The simulations were run on COSMOS, a 152 Gb shared memory Altix 3700 with 152 CPUs hosted at the Department of Applied Mathematics and Theoretical Physics (Cambridge).

In order to check the impact of a WDM particle on the flux power spectrum, we have run a set of simulations with different WDM particle masses and compared them with a ΛCDM simulation with the same phases of the initial conditions. The cosmological parameters for both simulations are $\Omega_{\mathrm{M}} = 0.26$, $\Omega_{\Lambda} = 0.74$, $\Omega_{\mathrm{B}} = 0.0463$, and $H_0 = 72\ \mathrm{km\ s^{-1}\ Mpc^{-1}}$. The ΛCDM transfer functions have been computed with CMBFAST [15]. The transfer function for the WDM model has been adopted from [7]. The simulations were run with a box size of 30 comoving h^{-1} Mpc with 2×200^3 gas and dark matter particles.

In Fig. 2 we show the fractional difference between the flux power spectra of a ΛWDM model and that of a ΛCDM model for a range of WDM particle masses at $z = 2.5, 3, 4$. The free streaming of the WDM particles has little effect for particles with masses $\gtrsim 1$ keV (thermal WDM) at scales for which the linear matter power spectrum can be reliably inferred (less than 5% at $z = 2.5$ increasing to 15% at $z = 4$). For smaller masses of the WDM particle there is, however, a dramatic reduction of the flux power spectrum. Note that at small scales $\lesssim 0.1 s/\mathrm{km}$, the flux power spectrum shows a bump. This is the effect of the nonlinear evolution of the matter distribution which results in a transfer of power from large scales to small scales [10]. The diamonds in Fig. 2 show the effect of adding randomly oriented velocities drawn from a Fermi-Dirac distribution in the initial conditions for the model with $m_{\mathrm{WDM}} = 1$ keV. We confirm the result of [10] that the effect of adding these free-streaming velocities on the flux power spectrum is small, of the order of 2% for $k < 0.03 s/\mathrm{km}$. We will neglect the effect in the following.

Figs. 1 and 2 suggest that the Lyman-α forest data will provide a tight lower limit to the mass of WDM particles. We will quantify this limit in the next section using the

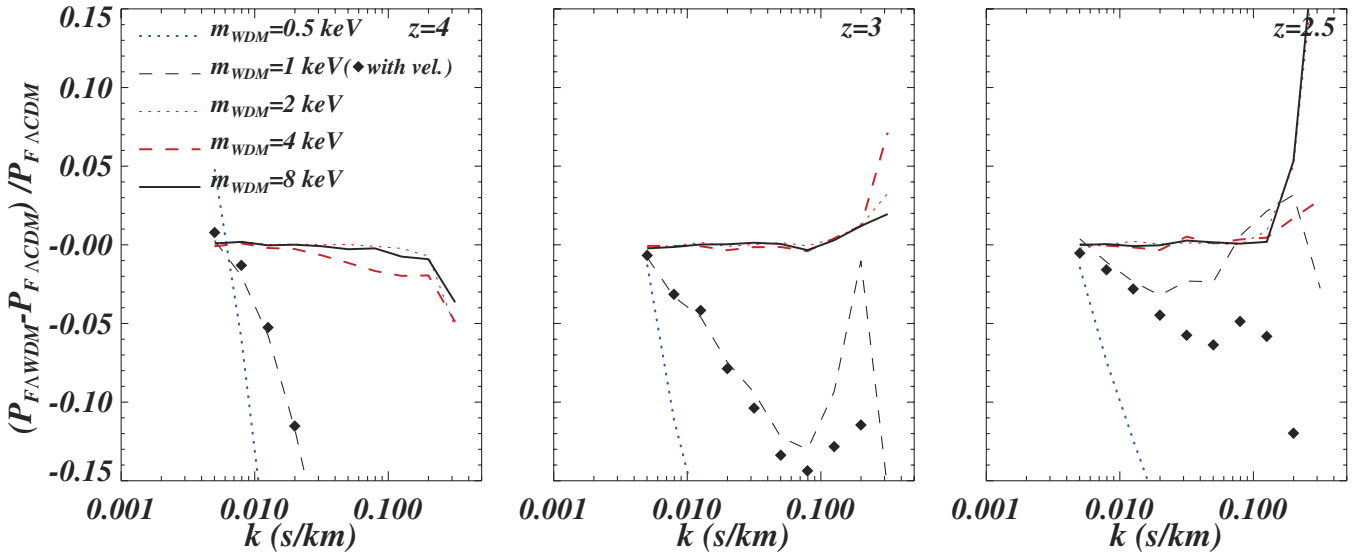

FIG. 2 (color online). Fractional difference of the flux power spectrum for a hydrodynamical simulation of a ΛWDM model and the flux power spectrum for a ΛCDM model. The simulations have a box size of $30h^{-1}$ Mpc and 200^3 gas and 200^3 dark matter particles. The results are for three different redshifts ($z = 4$, 3, 2.5, respectively, from left to right) and for five different values of the (thermal WDM) particle mass: 0.5 keV (thick dotted line), 1 keV (thin dashed line), 2 keV (thin dotted line), 4 keV (thick dashed line), and 8 keV (continuous line). The diamonds show the results for a simulation with a WDM particle of mass 1 keV when random oriented velocity dispersion drawn from a Fermi-Dirac distribution have been added in the initial conditions.

linear dark matter power spectrum in the range $(0.003\text{-}0.03)s/\mathrm{km}$ as inferred by VHS. We thereby checked how strongly the bias function used to infer the linear matter power spectrum depends on the presence of WDM. For this purpose we have run a simulation with a $60h^{-1}$ comoving Mpc box with 2×400^3 gas and warm dark matter particles for a (thermal WDM) particle mass $m_{\mathrm{WDM}} = 1$ keV. In the relevant wave number range, the difference between the bias function extracted from this simulation and that of a ΛCDM model (B2 model in VHS) is less than 3%, as we can see from Fig. 3. For smaller WDM particle masses the difference is expected to become larger but as we discuss in Section IV A this will have little impact on our final results.

C. Systematics Errors

There is a number of systematic uncertainties and statistical errors which affect the inferred power spectrum and an extensive discussion can be found in [12,13,29]. VHS estimated the uncertainty of the overall *rms* fluctuation amplitude of matter fluctuation to be 14.5% with a wide range of different factors contributing.

In the following we present a brief summary. The effective optical depth, $\tau_{\mathrm{eff}} = -\ln\langle F\rangle$ which is essential for the calibration procedure has to be determined separately from the absorption spectra. As discussed in VHS, there is a considerable spread in the measurement of the effective optical depth in the literature. Determinations from low-resolution low S/N spectra give systematically higher values than high-resolution high S/N spectra. However, there

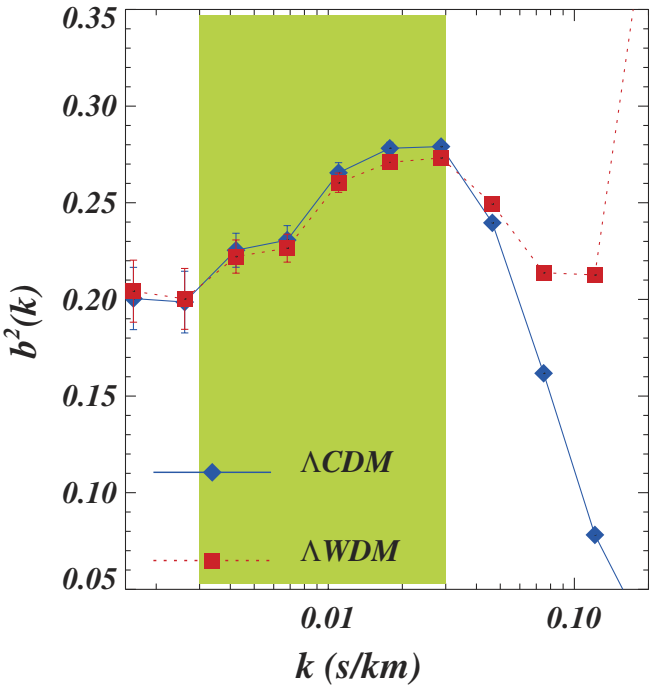

FIG. 3 (color online). Bias function $b^2(k)$ between the flux power spectrum and the linear dark matter power spectrum, $P_F(k) = b^2(k)P(k)$, for two cosmological models: ΛCDM (diamonds) and ΛWDM (squares), with a (thermal WDM) particle mass $m_{\mathrm{WDM}} = 1$ keV. The simulation has a box size of 60 comoving h^{-1} Mpc and 2×400^3 (gas and dark matter) particles (see Section III B for further details on other simulation parameters). The shaded area indicates the range of wave numbers used in our analysis.

is little doubt that the lower values from high-resolution high S/N spectra are appropriate and the range suggested in VHS leads to an 8% uncertainty in the *rms* fluctuation amplitude of the matter density field (Table 5 in VHS). Other uncertainties are the slope and normalization of the temperature-density relation of the absorbing gas which is usually parametrized as $T = T_0(1 + \delta_b)^{\gamma-1}$. T_0 and γ together contribute up to 5% to the error of the inferred fluctuation amplitude. VHS further estimated that uncertainties due to the C02 method (due to fitting the observed flux power spectrum with a bias function which is extracted at a slightly different redshift than the observations) contribute about 5%. They further assigned a 5% uncertainty to the somewhat uncertain effect of galactic winds and finally an 8% uncertainty due the numerical simulations (codes used by different groups give somewhat different results). Summed in quadrature, all these errors led to the estimate of the overall uncertainty of 14.5% in the *rms* fluctuation amplitude of the matter density field.

For our analysis we use the inferred DM power spectrum in the range $0.003\text{s/km} < k < 0.03\text{s/km}$ as given in Table 4 of VHS. Note that we have reduced the values by 7% to mimic a model with $\gamma = 1.3$, the middle of the plausible range for γ [32]. Unfortunately at smaller scales the systematic errors become prohibitively large mainly due to the large contribution of metal absorption lines to the flux power spectrum [13] (their Figure 3) and due to the much larger sensitivity of the flux power spectrum to the thermal state of the gas at these scales.

IV. BOUNDS ON THE WDM MASS FROM WMAP AND THE LYMAN-α FOREST

In this section we will show the results of our combined analysis of CMB data and Lyman-α forest data. The CMB power spectrum has been measured by the WMAP team over a large range of multipoles ($l < 800$) to unprecedented precision on the full sky [1]. For our analysis we use the first year data release of the WMAP temperature and temperature-polarization cross-correlation power spectrum.

For the range of parameters m_x and ω_x considered here, CMB anisotropies are not sensitive to the velocities of WDM particles and can therefore not discriminate between WDM and CDM models. It is nevertheless crucial to combine the CMB and Lyman-α data in order to get some handle on other cosmological parameters. Since all recent CMB experiments point toward a flat Universe with adiabatic scalar primordial fluctuations, we adopt these results as a prior. We treat the three ordinary neutrinos as massless (including small masses would not change significantly our results). We use the publicly available code CAMB [16] in order to compute the theoretical prediction for the C_l coefficients of the CMB temperature and polarization power spectra, as well as the matter spectrum $P(k)$. We derive the marginalized likelihood of each cosmological parameter with Monte Carlo Markov Chains as implemented in the publicly available code CosmoMC [33]. The calculations were performed on the Cambridge COSMOS supercomputer. We extended the CosmoMC package in order to include the Lyman-α forest data in a way similar to Ref. [34].

A. Lower bounds on m_x in a pure ΛWDM Universe

We first compute numerically the ΛCDM matter power spectrum, and then use Eq. (6) with $\nu = 1.2$ to obtain the pure ΛWDM matter power spectrum leaving the break scale α as a free parameter. Apart from α, our parameter set consists of the six usual parameters of the minimal cosmological model: the normalization and tilt of the primordial spectrum, the baryon density, the dark matter density $\omega_{\rm DM}$ (equal here to ω_x), the ratio of the sound horizon to the angular diameter distance, and the optical depth to reionization. Note that the Hubble parameter and the cosmological constant can be derived from these quantities, as well as σ_8 (the parameter describing the amplitude of matter fluctuations around the scale $R = 8h^{-1}$ Mpc). In addition to these seven cosmological parameters (with flat priors), we vary the parameter A (see [13,34]) which accounts for the uncertainty of the overall amplitude of the matter power spectrum inferred from the Lyman-α forest data (with a Gaussian prior as described in [34]).

The best-fit values for the cosmological parameters are summarized in the first column of Table I. In Fig. 4 (first panel), we show the marginalized likelihood for the break scale α. The probability peaks at $0.07h^{-1}$ Mpc, but the preference for a nonvanishing α is not statistically significant, and our main result is the upper bound $\alpha \lesssim 0.11h^{-1}$ Mpc at the 2σ confidence level. Using Eq. (7), we can derive the likelihood for the mass m_x, or better, for its inverse, in order to keep a nearly flat prior. The second panel of Fig. 4 shows the two-dimensional likelihoods for

TABLE I. The marginalized results for the recovered cosmological parameters for our WMAP + Lyman-α runs. The left column is for pure ΛWDM models while the second column is for mixed ΛCWDM models (with a fixed WDM temperature corresponding to $g_*(T_D) = 100$). The values correspond to the peaks of the marginalized probability distributions. Errors are the 68% confidence limits.

	ΛWDM	ΛCWDM
$\Omega_x h^2$	0.124 ± 0.015	0.149 ± 0.019
$\Omega_{\rm B} h^2$	0.024 ± 0.001	0.024 ± 0.001
h	0.72 ± 0.06	0.71 ± 0.06
τ	0.18 ± 0.09	0.17 ± 0.08
σ_8	0.96 ± 0.08	0.86 ± 0.09
n	1.01 ± 0.04	1.00 ± 0.04
$\alpha(\text{Mpc}/h)$	0.06 ± 0.03	...
f_x	...	0.05 ± 0.04

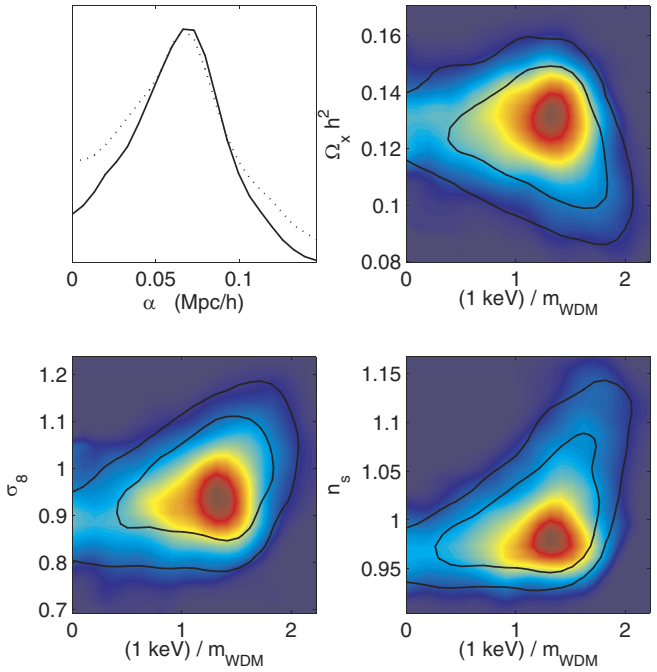

FIG. 4 (color online). Results for the pure ΛWDM model. The top left panel shows the likelihood for the break scale α. The other three panels show the 1σ and 2σ contours for (m_x^{-1}, ω_x), (m_x^{-1}, σ_8), and (m_x^{-1}, n_s), respectively, where m_x is the mass of a *thermal* WDM particle. The solid curves correspond to the full marginalized likelihoods, while the dashed curves and color/shade levels show the mean likelihood of the samples in the Markov chains.

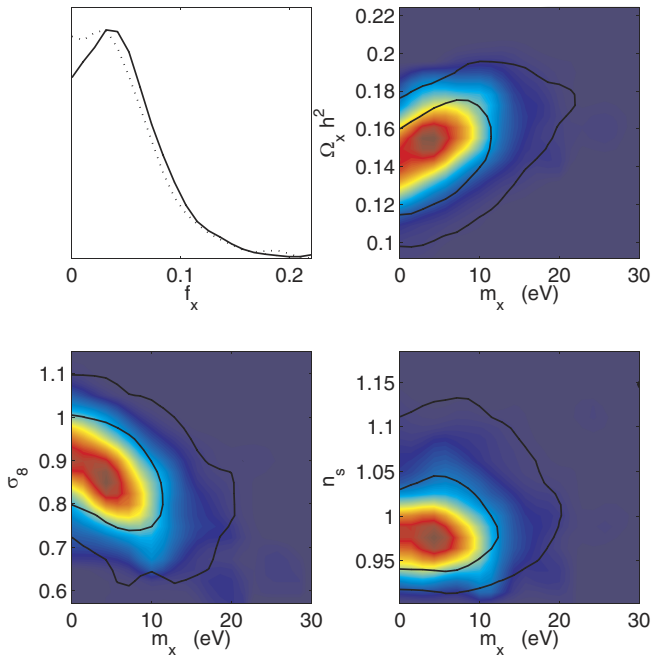

FIG. 5 (color online). Results for the ΛCWDM model with a light gravitino (or a particle decoupling when $g_* = 100$). The top left panel shows the likelihood for the WDM density fraction f_x. Other panels show the two-dimensional contours for the gravitino mass m_x and the most correlated variables: σ_8, n_s, and ω_X. The solid curves correspond to the full marginalized likelihoods, while the dashed curves and color/shade levels show the mean likelihood of the samples in the Markov chains.

the WDM parameters (m_x^{-1}, ω_x), assuming the WDM is a thermal relic. In this case the 2σ bound on the mass is $m_x \gtrsim 550$ eV, while for a nonthermal sterile neutrino as described in Section II this limit translates into $m_x \gtrsim 2.0$ keV.

Note that for particle masses $\lesssim 0.5$ keV the difference of the linear matter power spectrum of a WDM model compared to that of the corresponding CDM model are not small anymore at the relevant scales (Fig. 1). This makes the use of the linear bias relation as described in Section III questionable when deriving the likelihoods. The sensitivity to the mass of the WDM particle is however so strong that this should have no effect on our conclusions other than a possible small shift of our 1 and 2 σ bounds in this region.

We find no strong correlation between the mass of the WDM particle and other cosmological parameters. This is expected as the characteristic break due to the free-streaming length of the WDM particles cannot be easily mimicked by the effect of other parameters. Note however that the constraints on $\Omega_x h^2$, σ_8, and the tilt n_s of the primordial spectrum are significantly weakened for WDM particle masses $\lesssim 1$ keV and that somewhat larger values of σ_8 and n_s become allowed.

B. Upper bound on m_x in a ΛCWDM Universe

Let us now perform a similar analysis for the second model described in Section II: a ΛCWDM Universe with a warm thermal relic assumed to decouple when the number of degrees of freedom was $g_* = 100$ (as for instance for a light gravitino playing the role of the LSP). We choose the same set of cosmological parameters as in the previous subsection, except that the WDM sector is not described by the scale α but by the density fraction $f_x = \omega_x/\omega_{\rm DM}$ (where $\omega_{\rm DM} = \omega_x + \omega_{\rm CDM}$). The mass m_x is proportional to the density ω_x (Eq. (8)), and the limit $m_x \longrightarrow 0$ corresponds to the standard ΛCDM model. In this case, we will therefore obtain an upper instead of a lower limit on the mass.

In Fig. 5 (first panel), we show the marginalized likelihood for the WDM fraction. The 2σ Bayesian confidence limit $f_x \lesssim 0.12$ can be translated into a limit on the mass, $m_x \lesssim 16$ eV. The other three panels show two-dimensional contours for m_x and the most correlated variables: σ_8, ω_X, and n_s. There is now some correlation between the mass and the total dark matter density, because increasing $\omega_{\rm DM}$ tilts the small-scale matter power spectrum in such a way that it compensates to some extent the red tilting introduced by m_x. For the same reason, one could

expect some correlation with the tilt of the primordial spectrum. This does not occur because the value of the tilt is fixed more precisely than that of $\omega_{\rm DM}$ by the CMB data. The gravitino model predicts globally less power on small scales than ΛCDM. It therefore prefers smaller values of σ_8 in a combined analysis with the CMB data on large scales. Precise independent measurements of σ_8 could thus at least in principle tighten the limit on the mass of a putative gravitino.

Note that in this analysis, we assumed $g_*(T_D) = 100$, while as mentioned in Section II detailed studies of realistic supersymmetric models predict $87 < g_*(T_D) < 104$, for the mass range investigated here [18]. We have repeated our analysis assuming $g_*(T_D) = 90$ (which results in a slightly smaller coefficient of proportionality between the WDM mass and density) and found no significant difference.

V. CONCLUSIONS

We have obtained constraints on the mass of thermal and nonthermal WDM particles using a combined analysis of the cosmic microwave background data from WMAP and the matter power spectrum inferred from a large sample of Lyman-α forest data.

Assuming that the dark matter is entirely in the form of warm thermal relics, we find a 2σ upper bound $m_x \gtrsim 550$ eV on the mass of the DM particle. This confirms the result of Ref. [10] who got a slightly bigger lower limit. We have used a significantly larger sample of QSO spectra, applied an improved analysis which used state-of-the-art hydrodynamical simulations and taken into account a wide range of systematic uncertainties giving us confidence that our result is robust. Pushing this lower limit to larger masses will require accurate modeling of the Lyman-α forest data at smaller scales. This is difficult due to the sensitivity of the flux power spectrum to metal absorption and the thermal history of the gas at these scales.

It is interesting to compare this bound with those obtained from other methods. It has been noticed that reionization at $z \sim 6$ requires $m_{\rm WDM} \gtrsim 1$ keV, in addition if Swift discovers $z \sim 10$ gamma ray bursts then this would require even more stringent lower limits [36].

For nonthermal WDM particles like e.g. a sterile neutrino (with the same phase-space distribution as that of a standard neutrino, modulo a global suppression factor) this limit translates into $m \gtrsim 2.0$ keV (2σ). Note that in this case there exists also an upper bound $m \lesssim 5$ keV, from limits on the sterile neutrino decay rate in dark matter halos set by X-ray observations [35]. The existence of a WDM particle with a mass not much larger than these limits would increase the inferred amplitude of the matter power spectrum σ_8 and the inferred tilt of the primordial spectrum compared to a CDM cosmology.

Our results can be easily converted into a bound on a possible tiny interaction between CDM and photons, using the analysis of Ref. [37] (who showed that such an interaction would affect structure formation in the same way as WDM).

We have also obtained constraints on the mass of thermal relics which decoupled at temperatures of the order of GeV or TeV and on their contribution to the total matter density. In this case the number of degrees of freedom in the Universe at the time of decoupling $g_*(T_D)$ was of order of 100 and the particles cannot make up all the dark matter in the Universe—otherwise they would have a mass of order 100 eV which would contradict the limit discussed above. A light gravitino is a prime example of such a particle and would only be viable if it coexisted with ordinary cold dark matter (or with another form of warm dark matter particle with significantly larger mass). In this case, for particles with $g_*(T_D)$ in the range from 90 to 100, we find a 2σ bound $m_x \lesssim 16$ eV. So, if the gravitino is the LSP, as suggested by gauge-mediated susy breaking scenarios, the susy breaking scale is limited from above,

$$\Lambda_{\rm susy} \simeq (\sqrt{3} m_{3/2} M_p)^{1/2} \lesssim 260 \text{ TeV}. \qquad (11)$$

This conclusion is robust and relevant for supersymmetry searching at future accelerator machines as LHC. Indeed, if we assume that after decoupling the gravitino background was enhanced by the decay of the Next-to-lightest Supersymmetric Particle (NSP), as it happens in some scenarios [38], the total density of gravitinos as well as their velocity dispersion can only be enhanced, making the bound even stronger. The only possible way to evade this bound on the susy breaking scale (still assuming that the gravitino is the LSP) would be to assume some entropy production after gravitino decoupling, as suggested in Refs. [39,40].

ACKNOWLEDGMENTS

We thank G. F. Giudice for getting us interested in setting a bound on the scale of supersymmetry breaking, as well as George Efstathiou, Steen Hansen, and Sergio Pastor for useful comments. This work is partly supported by the European Community Research and Training Network "The Physics of the Intergalactic Medium." The simulations were done at the UK National Cosmology Supercomputer Center funded by PPARC, HEFCE, and Silicon Graphics / Cray Research. M. V. thanks PPARC for financial support. J. L. thanks the University of Padova and INFN for supporting a six-month visit during which this work was carried out. M. V. thanks the Kavli Institute for Theoretical Physics in Santa Barbara, where part of this work was done, for hospitality during the workshop on "Galaxy-Intergalactic Medium Interactions."

[1] WMAP Collaboration, D. N. Spergel *et al.*, Astrophys. J. Suppl. Ser. **148**, 175 (2003); A. Kogut *et al.*, Astrophys. J. Suppl. Ser. **148**, 161 (2003); G. Hinshaw *et al.*, Astrophys. J. Suppl. Ser. **148**, 135 (2003); L. Page *et al.*, Astrophys. J. Suppl. Ser. **148**, 233 (2003); L. Verde *et al.*, Astrophys. J. Suppl. Ser. **148**, 195 (2003).

[2] SDSS Collaboration, M. Tegmark *et al.*, Phys. Rev. D **69**, 103501 (2004); P. Crotty, J. Lesgourgues, and S. Pastor, Phys. Rev. D **69**, 123007 (2004); U. Seljak *et al.*, astro-ph/0407372.

[3] S. Hannestad and G. Raffelt, J. Cosmol. Astropart. Phys. 04 (2004) 008.

[4] H. Pagels and J. R. Primack, Phys. Rev. Lett. **48**, 223 (1982); J. R. Bond, A. S. Szalay, and M. S. Turner, Phys. Rev. Lett. **48**, 1636 (1982).

[5] P. J. E. Peebles, Astrophys. J. **258**, 415 (1982); K. A. Olive and M. S. Turner, Phys. Rev. D **25**, 213 (1982); S. Dodelson and L. M. Widrow, Phys. Rev. Lett. **72**, 17 (1994); X. d. Shi and G. M. Fuller, Phys. Rev. Lett. **82**, 2832 (1999); A. D. Dolgov and S. H. Hansen, Astropart. Phys. **16**, 339 (2002); K. Abazajian, G. M. Fuller, and M. Patel, Phys. Rev. D **64**, 023501 (2001).

[6] S. Colombi, S. Dodelson, and L. M. Widrow, Astrophys. J. **458**, 1 (1996).

[7] P. Bode, J. P. Ostriker, and N. Turok, Astrophys. J. **556**, 93 (2001).

[8] B. Moore, T. Quinn, F. Governato, J. Stadel, and G. Lake, Mon. Not. R. Astron. Soc. **310**, 1147 (1999).

[9] V. Avila-Reese, P. Colin, O. Valenzuela, E. D'Onghia, and C. Firmani, Astrophys. J. **559**, 516 (2001).

[10] V. K. Narayanan, D. N. Spergel, R. Dave, and C. P. Ma, Astrophys. J. **543**, L103 (2000).

[11] T. S. Kim, M. Viel, M. G. Haehnelt, R. F. Carswell, and S. Cristiani, Mon. Not. R. Astron. Soc. **347**, 355 (2004).

[12] R. A. C. Croft *et al.*, Astrophys. J. **581**, 20 (2002).

[13] M. Viel, M. G. Haehnelt, and V. Springel, Mon. Not. R. Astron. Soc. **354**, 684 (2004).

[14] J. R. Bond, G. Efstathiou, and J. Silk, Phys. Rev. Lett. **45**, 1980 (1980).

[15] U. Seljak and M. Zaldarriaga, Astrophys. J. **469**, 437 (1996); CAMB Code Home Page, http://cmbfast.org.

[16] A. Lewis, A. Challinor, and A. Lasenby, Astrophys. J. **538**, 473 (2000); CAMB Code Home Page, http://camb.info.

[17] S. H. Hansen, J. Lesgourgues, S. Pastor, and J. Silk, Mon. Not. R. Astron. Soc. **333**, 544 (2002).

[18] E. Pierpaoli, S. Borgani, A. Masiero, and M. Yamaguchi, Phys. Rev. D **57**, 2089 (1998).

[19] H. Bi, Astrophys. J. **405**, 479 (1993); M. Viel, S. Matarrese, H. J. Mo, M. G. Haehnelt, and T. Theuns, Mon. Not. R. Astron. Soc. **329**, 848 (2002); M. Zaldarriaga, R. Scoccimarro, and L. Hui, Astrophys. J. **590**, 1 (2003).

[20] P. McDonald *et al.*, astro-ph/0407377.

[21] L. Hui, N. Y. Gnedin, and Y. Zhang, Astrophys. J. **486**, 599 (1997).

[22] N. Katz, D. H. Weinberg, and L. Hernquist, Astrophys. J. Suppl. Ser. **105**, 19 (1996).

[23] J. E. Gunn and B. A. Peterson, Astrophys. J. **142**, 1633 (1965); J. N. Bahcall and E. E. Salpeter, Astrophys. J. **142**, 1677 (1965).

[24] M. Rauch, Annu. Rev. Astron. Astrophys. **36**, 267 (1998).

[25] L. Hui and N. Gnedin, Mon. Not. R. Astron. Soc. **292**, 27 (1997); N. Y. Gnedin and L. Hui, Mon. Not. R. Astron. Soc. **296**, 44 (1998).

[26] P. McDonald *et al.*, astro-ph/0405013.

[27] http://www.ast.cam.ac.uk/~rtnigm/luqas.htm

[28] L. Hui, S. Burles, U. Seljak, R. E. Rutledge, E. Magnier, and D. Tytler, Astrophys. J. **552**, 15 (2001).

[29] N. Y. Gnedin and A. J. S. Hamilton, Mon. Not. R. Astron. Soc. **334**, 107 (2002).

[30] V. Springel, N. Yoshida, and S. D. M. White, New Astron **6**, 79 (2001).

[31] F. Haardt and P. Madau, Astrophys. J. **461**, 20 (1996).

[32] M. Ricotti, N. Y. Gnedin, and J. M. Shull, Astrophys. J. **534**, 41 (2000); J. Schaye *et al.*, Mon. Not. R. Astron. Soc. **318**, 817 (2000).

[33] A. Lewis and S. Bridle, Phys. Rev. D **66**, 103511 (2002); CosmoMC home p.: http://www.cosmologist.info.

[34] M. Viel, J. Weller, and M. Haehnelt, Mon. Not. R. Astron. Soc. **355**, L23 (2004).

[35] K. Abazajian, G. M. Fuller, and W. H. Tucker, Astrophys. J. **562**, 593 (2001).

[36] R. Barkana, Z. Haiman, and J. P. Ostriker, Astrophys. J. **558**, 482 (2001); A. Mesinger, R. Perna, and Z. Haiman, astro-ph/0501233 [Astrophys. J. (to be published)].

[37] C. Boehm, A. Riazuelo, S. H. Hansen, and R. Schaeffer, Phys. Rev. D **66**, 083505 (2002).

[38] S. Borgani, A. Masiero, and M. Yamaguchi, Phys. Lett. B **386**, 189 (1996).

[39] E. A. Baltz and H. Murayama, J. High Energy Phys. 05 (2003) 067.

[40] M. Fujii and T. Yanagida, Phys. Lett. B **549**, 273 (2002).